Revista de Metalurgia
Vol. 53, Issue 3, July–September 2017, e100
ISSN-L: 0034-8570
http://dx.doi.org/10.3989/revmetalm.100

Synthesis and investigation of BiSbTeSe single crystal doped with Zr produced using Bridgman method

Emina Požega[a,✉], Pantelija Nikolić[b], Slavko Bernik[c], Lidija Gomidželović[a], Nebojša Labus[b], Milan Radovanović[d], Saša Marjanović[e]

[a] Mining and Metallurgy Institute Bor, Zeleni Bulevar 35, 19210 Bor, Serbia
[b] Institute of Technical Sciences of SASA, Knez Mihailova 35/IV, 11000 Belgrade, Serbia
[c] Jožef Stefan Institute, Jamovacesta 39, 1000 Ljubljana, Slovenia
[d] Faculty of Technical Sciences, University of Novi Sad, Trg Dositeja Obradovića 6, 21000 Novi Sad, Serbia
[e] University of Belgrade, Technical Faculty Bor, VJ 12, 19210 Bor, Serbia
(✉Corresponding author: emina.pozega@irmbor.co.rs)

Submitted: 22 June 2016; Accepted: 25 April 2017; Available On-line: 13 September 2017

ABSTRACT: Single crystal ingot of BiSbTeSe doped with Zr was synthesized using Bridgman method. Energy dispersive spectrometry (EDS) analysis was used to determine chemical composition of studied samples as well as to check and confirm samples homogeneity. X-ray diffraction (XRD) measurements proved that obtained crystal ingot is a single cristal and confirms Bi_2Te_3-type compound with orientation (00l) of single crystal. Melting point was determined by dilatometrically measured shrinkage during heating. Mobility, concentration, resistivity/conductivity and Hall coefficient of BiSbTeSe doped with Zr samples were determined using a Hall Effect measurement system based on the Van der Pauw method. The Hall Effect was measured at room temperature with an applied magnetic field strength of 0.37 T at different current intensities. The measured ingot samples were cut and cleaved from different regions. Calculated results obtained using a Hall Effect measurement system (Ecopia, HMS-3000) were mutually compared for cleaved and cut samples. Changing of transport and electrical parameters with the increase of the current intensity was also monitored.The results confirmed that electrical and transport properties of single crystal depend on crystal growth direction and mobility was also significantly improved in comparison with theoretical value of Bi_2Te_3 and available literature data.

KEYWORDS: Bridgman method; Dilatometric analysis; EDS; Hall Effect measurement system; Single crystal; XRD

Citation/Citar como: Požega, E.; Nikolić, P.; Bernik, S.; Gomidželović, L.; Labus, N.; Radovanović, M.; Marjanović, S. (2017) "Synthesis and investigation of BiSbTeSe single crystal doped with Zr produced using Bridgman method". *Rev. Metal.* 53(3):e100. http://dx.doi.org/10.3989/revmetalm.100

RESUMEN: *Síntesis e investigación del mono cristal BiSBTeSe dopado con Zr obtenido mediante el método de Bridgman*. El lingote del mono cristal de BiSbTeSe dopado con Zr se sintetizó utilizando el método de Bridgman. La composición química se determinó mediante análisis con espectroscopía de dispersión de energía (EDS). Mediante difracción de rayos X (DRX) se demostró que el lingote de cristal obtenido es un mono cristal y confirmó que se trata de un compuesto del tipo Bi_2Te_3, con orientación del mono cristal (001). El punto de fusión se determinó por medidas dilatométricas. La movilidad, concentración, resistividad/conductividad, y el coeficiente de Hall del BiSbTeSe dopado con Zr, se determinaron utilizando un sistema de medición de efecto Hall basado en el método de Van der Pauw. El efecto Hall se midió a temperatura ambiente con una intensidad de campo magnético aplicada de 0,37 T a diferentes intensidades de corriente. Las muestras de lingotes medidos se cortaron y se rompieron de diferentes regiones.

Las muestras de lingotes utilizadas en las medidas fueron obtenbidas mediante corte y escisión en distintas zonas. Los resultados obtenidos utilizando un sistema de medición de efecto Hall (Ecopia, HMS-3000) en las distintas muestras, se compararon entre sí. Los resultados confirmaron que las propiedades eléctricas y de transporte del mono cristal dependen de la dirección del crecimiento del cristal. La movilidad se mejoró significativamente en comparación no solo con el valor teórico de Bi_2Te_3 sino también con los datos existentes en la literatura.

PALABRAS CLAVE: Análisis dilatométrico; EDS; Método Bridgman; Monocristal; Sistema de medición de efecto Hall; XRD

ORCID ID: Emina Požega (http://orcid.org/0000-0001-6797-2435); Pantelija Nikolić (http://orcid.org/0000-0002-2196-4736); Slavko Bernik (http://orcid.org/0000-0001-7330-3094); Lidija Gomidželović (http://orcid.org/0000-0002-0783-0328); Nebojša Labus (http://orcid.org/0000-0003-1557-0711); Milan Radovanović (http://orcid.org/0000-0002-9702-3879); Saša Marjanović (http://orcid.org/0000-0001-6930-2232)

1. INTRODUCTION

Bismuth telluride was widely studied as a thermoelectric material, particularly in temperature range around 27 ºC (Fleurial *et al.*, 1988) Jariwala *et al.*, 2015). Bi_2Te_3 has useful application in the field of thermoelectric devices as solid state coolers for cooling of electronic components and in space technology for military purposes (Požega *et al.,* 2015), like generators Bi_2Te_3 have found application in space craft. Therefore, studies on various properties of bismuth telluride are interesting for both basic and applied research. Thermoelectric performance of Bi_2Te_3 is characterized by dimensionless figure of merit, ZT. Study of bismuth telluride showed a sharp maximum in figure of merit as a function of stoichiometric deviation (Fleurial *et al.*, 1988). Doping of semiconducting compounds is largely used as a method of controlled synthesis. Transport property measurements in doped Bi_2Te_3 single crystals with Se and Fe have been studied by measuring the thermoelectric power and electrical conductivity in the temperature range 30 ºC to 200 ºC (Jariwala *et al.*, 2015). They focused on improving the transport properties by better control of the stoichiometry through a uniform impurity distribution during the growth process.Se doped Bi_2Te_3 single crystals have been reported to be thermoelectric materials with maximum figure of merit, ZT~1.04 at 125 ºC (Yan *et al.*, 2010; Soni *et al.*, 2012; Guo *et al.*, 2014; Jariwala *et al.*, 2015). $(BiSb)_2(TeSe)_3$belongs to the family of narrow-band semiconductors $A_2^{V}B_3^{VI}$ (A = Bi, Sb and B = Te, Se) with the tetradymite structure (Kašparová *et al.*, 2005; Rowe, 2005). All semiconductors of the general formula $(BiSb)_2(TeSe)_3$ are solid solutions, which are isostructural with the Bi_2Te_3. They have layered structure of Bi_2Te_3 type. Layered structure of Bi_2Te_3 compound is a result of much stronger interatomic bonds between Te atoms in a plane layer of the same bond between layers.The reduction in the lattice component of thermal conductivity, λ_L can be achieved through the use of solid solutions (Rosi *et al.,* 1959) of bismuth telluride with the isomorphous compounds antimony telluride and bismuth selenide (Goldsmid, 2014). Also improvement of power factor ($\alpha^2\sigma$), where α is Seebeck coefficient, σ is the electrical conductivity, can be obtained by the adoption of nanostructures (Goldsmid, 2014).Transport properties of the quaternary systems of BiSbTeSe have been measured as function of temperature in the temperatura range of 27 ºC to 227 ºC (Farag *et al.*, 2010). They obtained a concentration of majority charge carriers of 10^{19} cm^{-3}. Problem of optimizing impurity content of bismuth telluride alloys for specific temperatures were studied (Rowe, 2005). Generator materials up to 800 ºC have been reviewed, specifying $Bi_2Se_{0.6}Te_{2.4}$ and $Bi_{0.5}$ $Sb_{1.5}Te_3$, as the n-type and p-type materials up to 300 ºC, but without discussing of carrier concentration optimization (Dashevsky *et al.,* 1997).The investigated properties of $Bi_{0.4}Sb_{1.6}Te_3$ with 0.3 wt% of PbTe showed that ZT rises from about 1.0 at 50 ºC to 1.1 at 107 ºC and then fell to 0.8 at 350 ºC (Kusano and Hori, 2002).The properties of n-type $Bi_xSb_{2-x}Te_3$, with x between 0.5 and 0.7, were studied (Gerovac *et al.*, 2010). Mechanochemical synthesis of a nanocrystalline thermo electric compound were investigated and found that if the particle size is being reduced, structural defects will be increased and hence solid state chemical reactions will be enhanced (Rojas-Chávez *et al.,* 2010). Various investigations were performed improvement of thermoelectric performance of Bi_2Te_3 alloy, too (Wu *et al.,* 2013).

In this paper BiSbTeSe doped with Zr was investigated. Attention was paid to the improvement of the electrical performance of BiSbTeSe. After review of available literature data, it has been concluded that this type of multi-component material has not been synthesized and studied until now.

2. MATERIALS AND METHODS

Single crystal ingot of BiSbTeSe doped with Zr was synthesized using the Bridgman method at the maximum temperature of 600 ºC. High purity elements (5 N and 6 N) were used as the source material. Bismuth (Sigma-Aldrich, 99.999%), antimony shot

(Koch Light Labaratories LTD, 99.9999%), selenium shot (Alfa Aesar, 99.999%) and tellurium (Sigma-Aldrich, 99.999%) were taken in determined proportion and sealed in quartz ampoule under pressure of 10^{-5} Pa. Zirconium (KEFO) was of 99.98% purity. Quartz ampule was lowered at a speed of 2.2 mmh^{-1} in the field of vertical furnace (Nikolić *et al.*, 2010; Dordević *et al.,* 2012). A slow rate of crystallization was desirable to avoid the internal stresses and microcracks. P type single crystal sample was synthesized in a vertical configured furnace with very precise temperature regulation. Single crystal of Zr doped BiSbTeSe with dimensions of 80 mm in length and 9.2 mm in diameter were obtained. Obtained ingot was cut into plates with dimensions of 2.2 mm and cylinders with 9 mm in length. Cylinders were cleaved longitudinally in order to obtain square shape plates with thickness between 1.5 to 2 mm and with very flat and glossy surface. Quartz ampoule had the conical shape in the bottom for easier formation of seed. The inside of the ampoule was protected in order to prevent contact between the growing sample and quartz ampoule wall. Analyses of samples composition were performed by an energy dispersive spectroscopy (EDS), type Oxford Inca 3.2, coupled with the scanning electron microscope Jeol JSM 5800, operated at 20 keV. X-ray intensity measurement was carried out on a PHILIPS PW 1710 automated diffractometer using monochromatized Cu Kα radiation. Melting point of the sample was determined on the dilatometer Bähr GmbH Thermoanalyse 802 s. Dilatometric analyses were carried out under following conditions: air atmosphere, heating rate 10 $^{o}Cmin^{-1}$ and Tmax = 600 °C. Rectangle cross-section sample with dimensions 7.74x4.82 mm with thicknes of 1.71 mm was used for the investigations. Al_2O_3, with dimensions 2x1.26 mm and l0 of 0.45 mm, was used as a reference material. Hall measurements were performed on a Hall Effect measurement system (Ecopia, HMS-3000) at room temperature and different electric currents intensities for the applied magnetic field of 0.37 T. Software program of Hall Effect measurement system (Ecopia, HMS-3000) automatically calculated bulk and sheet carrier concentration, specific resistance, conductivity and Hall coefficient. Calculations were done on the basis of voltage obtained by Van der Pauwlaws (Pauw Van der, 1958) and entered input data into the software (sample thickness *D*, current intensity *I*, the magnetic induction of permanent magnet *B*). Data from Hall measurements at room temperature were collected using Schottky diode contacts. The measured samples were cut and cleaved from different regions of the ingot, with cutting route perpendicular (⊥) and cleaved parallel (||) to the plane of crystallisation. In the following text these samples will be marked as 8/3 (⊥), 8/4 (⊥), 8/5 (||), 8/6 (⊥) and 8/8 (||), respectively. Samples cut perpendicular (⊥) to the growth of the ingot were in the form of discs and samples cleaved parallel (||) to the plane of crystallisation were square cross-section. Cut samples were then highly mechanically polished. The measured samples were cleaned in acetone before the measurements.

3. RESULTS AND DISCUSSION

3.1. Scanning electron microscopy with energy dispersive spectrometry (SEM-EDS)

Samples 8/5 (||) and 8/8 (||) were attached on the cut samples 8/3 (⊥), 8/4 (⊥) and 8/6 (⊥) since all the samples were from the same ingot. Therefore, energy dispersive spectrometry measurements were performed only on 8/5 (||) and 8/8 (||) samples to estimate composition of ingot.The experimental results of the samples 8/5 (||) and 8/8 (||) composition, done by energy dispersive spectrometry analysis, are presented in Table 1, where also the presence of Zr can be observed. The ingot top contains more zirconium, bismuth and tellurium, as shown in Table 1. At the end of the crystal there is more antimony and selenium. Based on energy dispersive spectrometry analysis it is observed a good homogeneity of single crystal composition with variation inside experimental error of energy dispersive spectrometry analysis.

3.2. X-ray diffraction analysis (XRD)

X-ray diffractogram for the single crystal of Zr doped BiSbTeSe sample is depicted in Fig. 1.Only Bragg reflections are given in this diffraction pattern. Using the values obtained for the lattice parameters of the Bi_2Te_3 compound and ASTM tables, it was calculated that these are Bragg reflections of the planes with Miller's indices (003), (006), (009), (0012), (0015) and (0018). Single crystal plate was cleaved, from the ingot, and Bragg's diffractions confirmed it orientation (00l).

3.3. Dilatometric analysis

Obtained temperature (572 ºC) on Fig. 2 is close to melting temperature of Bi_2Te_3 compound, but slightly decreased, which can be contributed to the presence of Se, Sb and Zr. Declared melting point helped us to determine the temperature which has to be passed during synthetitc heating. Also, high melting point of Zr was intriguing since it can be

TABLE 1. Representation of elements in samples in atm.% obtained by SEM-EDS analysis

Element / Sample	Bi	Sb	Te	Se	Zr
8/5 (||)	11.83	24.32	63.10	0.23	0.52
8/8 (||)	11.48	24.75	63.01	0.26	0.50

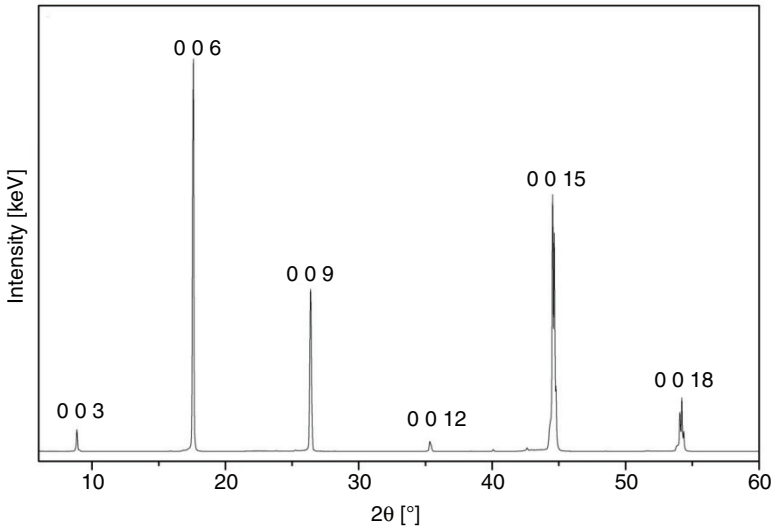

FIGURE 1. X-ray diffractogram of single crystal BiSbTeSe doped with Zr.

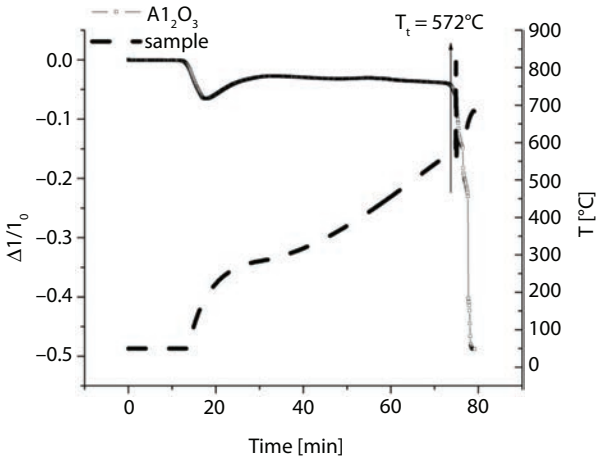

FIGURE 2. Dilatometric curve of Zr doped BiSbTeSe single crystal.

found in the form of oclusions in telluride phase. Energy dispersive spectrometry analysis proved that Zr aded as metal in zero valent state is incorporated in formed lattice of telluride.

3.4. Hall Effect measurements at room temperature

Hall Effect measurements at room temperature were carried out by passing a 0.1, 0.5, 1 and 5 mA current through the samples under magnetic field of 0.370 T. All calculated data from Hall measurements at room temperature for samples: 8/3 (⊥), 8/4 (⊥), 8/5 (||), 8/6 (⊥) and 8/8 (||) are presented in Figs. 3-8.

The results of specific resistance and conductivity are displayed in Figs. 3b, 4b, 5b, 6b and 7b. Figs. 3b, 4b, 5b, 6b and 7b show how resistivity and conductivity varies in the current range 0.1 – 5 mA. From these figures, it can be observed that specific resistivity is decreasing with the current intensity, i.e. electrical conductivity increases with the current intensity. Values of specific conductivity vary from 104 to 2615 $\Omega^{-1}cm^{-1}$and are higher for samples 8/5 (||) and 8/8 (||).The Hall Effect measurements show that the carrier concentration increases. The results are displayed in Figs. 3a, 4a, 5a, 6a and 7a, giving the bulk and sheet carrier concentration, as a function of the current intensity, A.

As shown in Fig. 3a, bulk and sheet carrier concentration for sample 8/3 (⊥) increases with the current intensity up to 1 mA. There after, bulk and sheet carrier concentration decreases. From Fig. 3b it can be observed that specific resistivity is decreasing with the current intensity increasing, i.e. electrical conductivity increases with the current intensity. Dependence of bulk and sheet carrier concentration from the current intensity for simple 8/4 (⊥) are displayed in Fig. 4a. Sheet carrier concentration is fairly constant and was found that is 10^{18} cm^{-2}. Bulk carrier concentrations at the current intensity of 0.1 mA and 0.5 mA are n_b = 1.889x10^{18} cm^{-3}, n_b = 1.034x10^{19} cm^{-3} respectively. At the current intensity of 1 mA bulk carrier concentration decreases to value of 8.583x10^{18} cm^{-3}. Thereafter bulk carrier concentration increases as the current intensity increases. The specific resistance of sample 8/4 (⊥) shown in Fig. 4b decreases as the current intensity increases from 0.1 to 1 mA and after that specific resistance increases. The plot of the specific conductivity dependence from the current intensity for sample 8/4 (⊥) is shown in the Fig. 4b. As it can been seen the specific conductivity increases as the current intensity increases from 0.1 to 1 mA. At the current intensity of 1 mA specific conductivity is σ = 5.559x10^2 $\Omega^{-1}cm^{-1}$. After that specific conductivity decreases. Dependence of bulk and sheet carrier concentration from the current intensity for

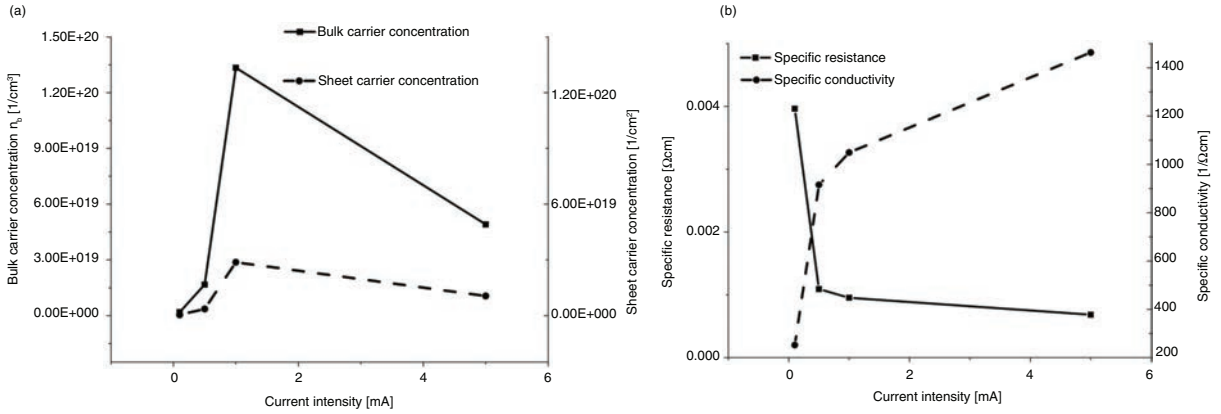

FIGURE 3. Dependence of: (a) bulk and sheet carrier concentration and (b) specific resistance and conductivity from current intensity for sample 8/3 (⊥) at room temperature.

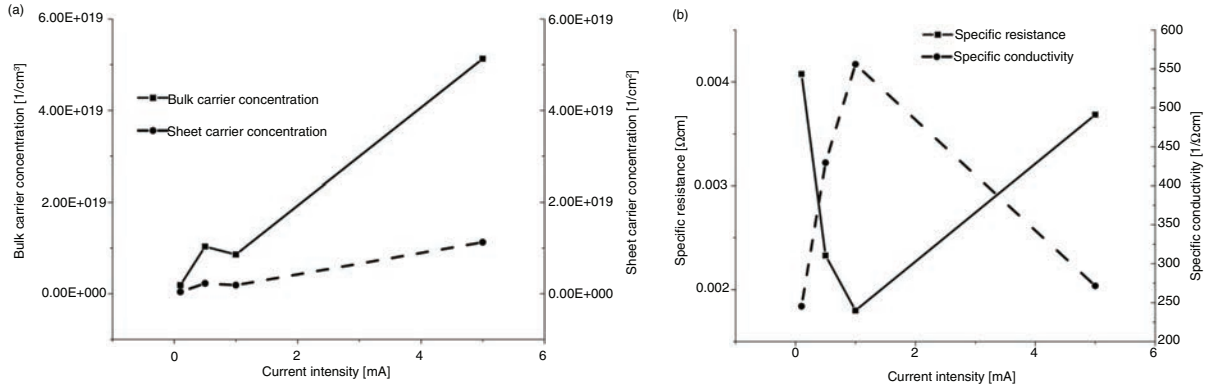

FIGURE 4. Dependence of: (a) bulk and sheet carrier concentration and (b) specific resistance and conductivity from current intensity for sample 8/4 (⊥) at room temperature.

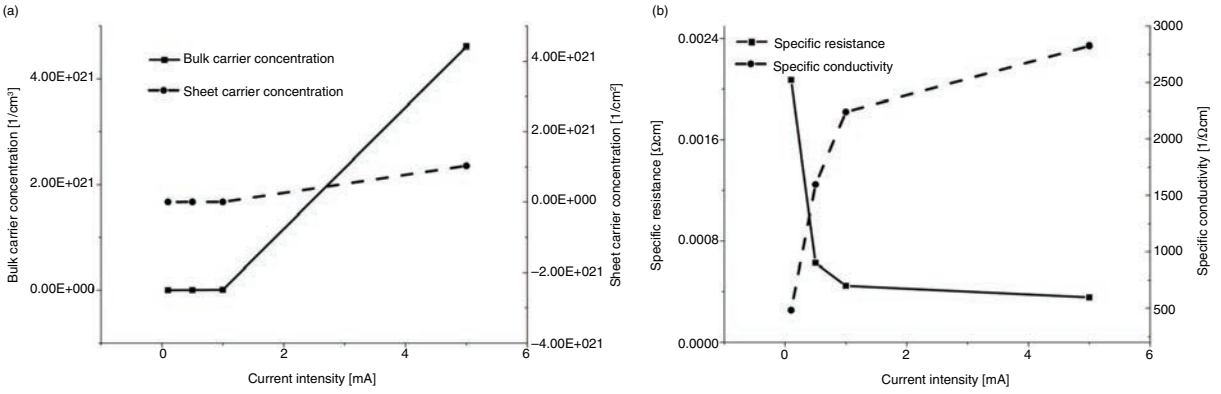

FIGURE 5. Dependence of: (a) bulk and sheet carrier concentration and (b) specific resistance and conductivity from current intensity for sample 8/5 (||) at room temperature.

sample 8/5 (||) is displayed in Fig. 5a. Bulk and sheet carrier concentration are fairly constant in range of 0.1 – 1 mA. The diagram show that bulk and sheet carrier concentrationare in the range of 10^{17} – 10^{20} cm^{-3}. Power factor is related to carrier concentration and is maximized at n ~ 10^{20} cm^{-3} in semiconductors (Snyder and Toberer, 2008). On Fig. 5b is displayed dependence of specific resistance and conductivity from the current intensity for simple 8/5 (||). It may be noted that the specific resistance decreases as the current intensity increases and is fairly constant in range of 1–5 mA. Specific conductivity increases as the current intensity increases. Dependence of bulk and sheet carrier concentration

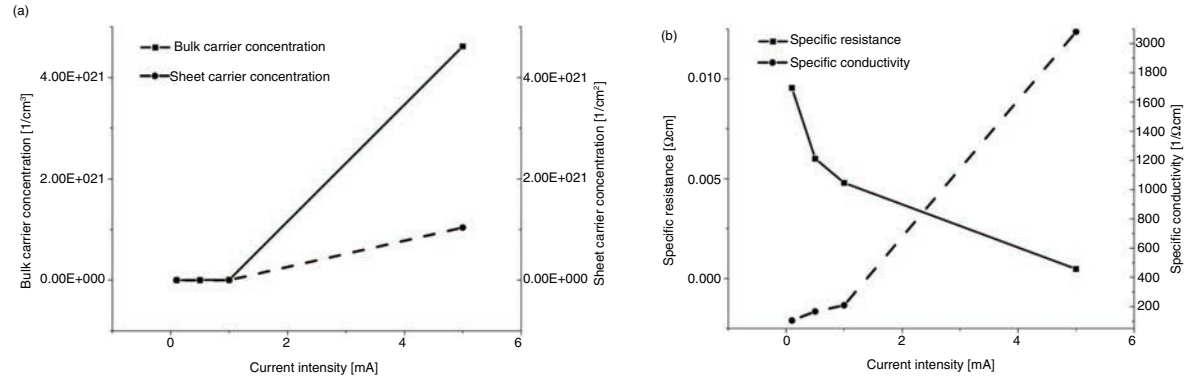

FIGURE 6. Dependence of; (a) bulk and sheet carrier concentration and (b) specific resistance and conductivity from current intensity for sample 8/6 (⊥) at room temperature.

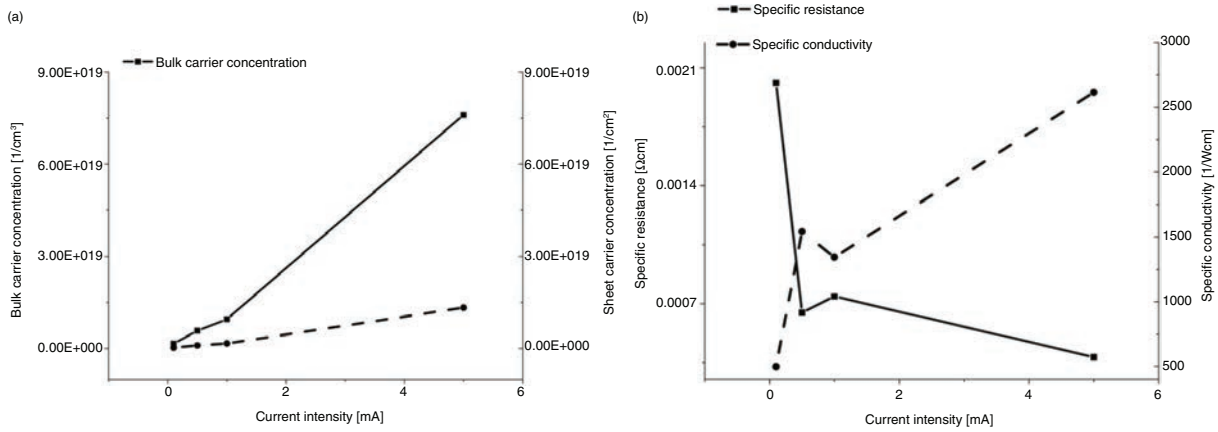

FIGURE 7. Dependence of: (a) bulk and sheet carrier concentration and (b) specific resistance and conductivity from current intensity for sample 8/8 (||) at room temperature.

from the current intensity for sample 8/6 (⊥) are displayed in Fig. 6a. Bulk and sheet carrier concentration are fairly constant in range of 0.1–1 mA. As it can be seen from Fig. 6b the specific conductivity increases and the specific resistanceof simple 8/6 (⊥) decreases as the current intensity increases. Bulk and sheet carrier concentration for simple 8/8 (||) increases with the current intensity (Fig. 7a). The results of specific resistance and conductivity dependence from the current intensity for sample 8/8 (||) are show in Fig. 7b. We see that the resistance decreases (except for current intensity of 1 mA) with the current intensity, showing metallic character of the material. A little deviation in derived measurement results of specific resistance, conductivity, bulk and sheet carrier concentration can be contributed to interval time between measurements.

The variation of Hall coefficient R_H with the current intensity for all samples is shown in Fig. 8a. Values of Hall coefficient are positive for all samples and decreases with current. It means that our single crystal is p-type in nature and majority charge carriers are holes. This can be support by Seebeck coefficient measurements (Deshpande *et al.,* 2009).

A change in carrier mobility with the current increase is also researched. The cleaved samples 8/5 (||) and 8/8 (||) had highest mobility of free carriers-holes.

As shown on Fig. 8b mobility calculated from Hall measurements was found to decrease with the increase of the current intensity for all samples. In this case, the mobility for the samples 8/5 (||) and 8/8 (||) is higher than theoretical value for Bi_2Te_3 which is 510 $cm^2V^{-1}s^{-1}$(Gol'cman *et al.,* 1972). It is about a factor of 4 better for samples 8/5 (||) and 8/8 (||) than theoretical value for Bi_2Te_3.

4. CONCLUSIONS

- BiSbTeSe single crystal doped with Zr was successfully synthesized. XRD analysis confirmed Bi_2Te_3 structure and (00l) orientation. Scanning electron microscopy with energy dispersive spectrometry (SEM-EDS) indicates that single crystal has a homogeneous composition.
- The content of Bi, Sb, Te, Se and Zr in samples was obtained using Energy Dispersive X-ray Spectroscopy (EDS) analysis. Along the ingot,

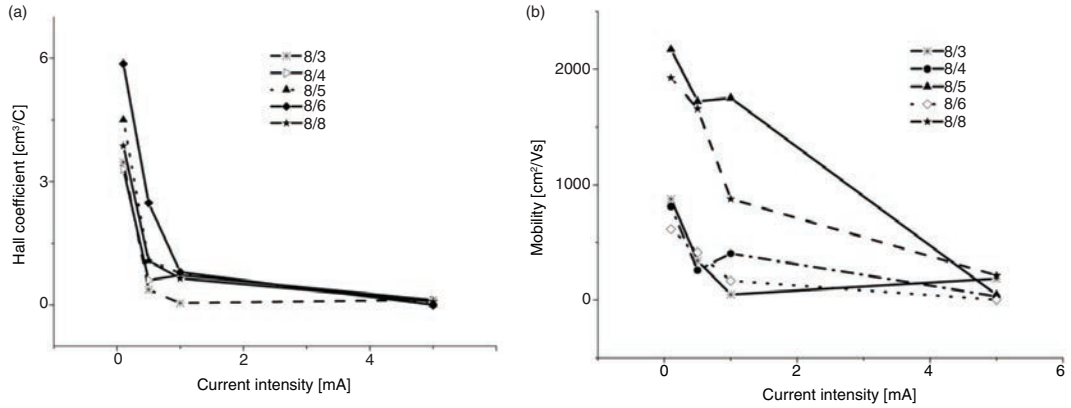

FIGURE 8. The variation of: (a) Hall coefficient R_H and (b) mobility with current for samples: 8/3 (⊥), 8/4 (⊥), 8/5 (||), 8/6 (⊥) and 8/8 (||) at room temperature.

the concentration of Zr decreased from the top to the end of the ingot. Bragg's diffractions confirmed orientation (00l) for cleaved sample. Melting point is determined using dimensions from graphics change in function of time (Fig. 2). The results of Hall measurements in two different directions on high quality single crystal obtained by standard Bridgman method were presented. Measurements were taken in the direction of crystal growth and normal to the direction of crystal growth.

– Using the Hall Effect measurement system, it was proved that all samples were of the "p" type with high carrier mobility of 10^3 cm^2Vs^{-1} at 25 °C and high carrier concentration of 10^{19} cm^{-3}. Mobility varies from $2.173x10^3$, $1.723x10^3$, $1.752x10^3$ and $4.648x10^1$ for sample *8/5 (||)*. For sample *8/8 (||)* mobility is in range $1.926x10^3$ - $2.146x10^2$ cm^2Vs^{-1}. Measurements of single crystal electrical properties confirmed their high quality and potential for practical application.

ACKNOWLEDGMENTS

Author wishes to thank Stevan Vujatović for manufacturing high-quality monocrystalline ingots and Dr. Dorđe Veljović for his assistance in the characterization of samples. The authors are grateful to the Ministry of Education, Science and Technological Development of the Republic of Serbia for financial support of project: "Development of ecological knowledge-based advanced materials and technologies for multifunctional application" (Grant Nº TR34005).

REFERENCES

Dashevsky, Z., Drabkin, I., Korotaev, V., Rabinovich, D. (1997). Improved materials for thermoelectric conversion (generation). *Proceedings of the 16th IEEE International Conference on Thermoelectrics*, Dresden, Free State, Germany, pp. 26–29.

Deshpande, M.P., Pandya, N.N., Parmar, M.N. (2009). Transport property measurements of Bi_2Se_3 crystal grown by Bridgman method. *Turk. J. Phys.* 33, 139–148. http://dx.doi.org/10.3906/fiz-0811-8.

Đordević, S.V., Wolf, M.S, Stojilović, N., Nikolić, M.V., Vujatović, S.S., Nikolić, P.M., Tung, L.C. (2012). Magneto–optical effects in semimetalic $Bi_{1-x}Sb_x$ (x = 0.015). *Phys. Rev. B*86 (11–15), 115119. https://doi.org/10.1103/PhysRevB.86.115119.

Farag, B.S., Abou el Soud, A.M., Zayed, H.A., Gad, S.A. (2010). Transport properties of the quaternary systems of Bi-Sb-Te-Se. *J. Ovonic Res.*6 (6), 267–275.

Fleurial, J.P., Gailliard, L., Triboulet, R., Scherrer, H., Scherrer, S. (1988). Thermal properties of high quality single crystals of bismuth telluride – part I: experimental characterization. *J. Phys. Chem. Solids*. 49 (10), 1237–1247. https://doi.org/10.1016/0022-3697(88)90182-5.

Gerovac, N., Snyder, G.J., Caillat, T. (2002). Thermoelectric properties of n-type polycrystalline Bi_xSb_{2-x} Te_3 alloys. *Proceedings of the 21st IEEE International Conference on Thermoelectrics*, Long Beach, CA, USA, pp. 25–29.

Goldsmid, H.J. (2014). Bismuth Telluride and Its Alloys as Materials for Thermoelectric Generation. *Materials*. 7(4), 2577–2592. http://dx.doi.org/10.3390/ma7042577.

Gol'cman, B.M., Kudinov, V.A., Smirnov, I.A. (1972).*Semiconductor thermoelectric materials based on Bi_2Te_3*. Moskva, Russian.

Guo, X., Jia, X., Jiang, Y., Sun, H., Zhang, Y., Sun, B., Liu, B., Ma, H. (2014*)*. Improved thermoelectric performance of $Bi_2Te_{3-x}Se_x$ bulk materials produced by the preparation of high-pressure. *Funct. Mater. Lett*. 7(5),1450051. http://dx.doi.org/10.1142/S1793604714500519.

Jariwala, B., Shah, D., Ravindra, N.M. (2015). Transport property measurements in doped Bi_2Te_3 single crystals obtained via zone melting method. *J. Electron. Mater*. 44 (6), 1509–1516. http://dx.doi.org/10.1007/s11664-014-3438-1.

Kašparová, J., Dražar, Ė., Krejèová, A., Beneš, L., Lošt'ák, P., Chen, W., Zhou, Z., Uher, C.(2005). n-type to p-type crossover in quaternary $Bi_xSb_yPb_2Se_3$ single crystals. *J. Appl. Phys.* 97(10), 103720–103725. http://dx.doi.org/10.1063/1.1904158.

Kusano, D., Hori, Y. (2002). Effects of PbTe doping on the thermoelectric properties of $(Bi_2Te_3)_{0.2}(Sb_2Te_3)_{0.8}$.*Proceedings of the 21st IEEE International Conference on Thermoelectrics*, Long Beach, CA, USA, pp. 25–29.

Nikolić, P.M., Vujatović, S.S., Ivetić, T., Nikolić, M.V., Cvetković, O., Aleksić, O.S., Blagojević, V., Branković, G., Nikolić, N. (2010).Thermal diffusivity of single crystal $Bi_{0.9}Sb_{0.1}$. *Sci. Sinter*. 42 (1), 45–50. http://dx.doi.org/10.2298/SOS1001045N.

Pauw Van der, L.J. (1958). A method of measuring the resistivity and Hall coefficient on lamellea of arbitrary shape. *Philips Tech. Rev.* 20, 220–224.

Požega, E., Ivanov, S., Stević,Z., Karanović, Lj., Tomanec, R., Gomidželović, L., Kostov, A. (2015). Identification and characterization of single crystal $Bi_2Te_{3-x}Se_x$ alloy. *T. Nonferr. Metal. Soc.* 25 (10), 3279–3285. http://dx.doi.org/10.1016/S1003-6326(15)63964-4.

Rojas-Chávez, H., Reyes-Carmona, F., Jaramillo-Vigueras, D. (2010). Mechanochemical synthesis of a nanocrystalline thermoelectric compound. *Rev. Metal*. 46 (6), 548–554. http://dx.doi.org/10.3989/revmetalmadrid.1020.

Rosi, F.D., Abeles, B., Jensen, R.V. (1959). Materials for thermoelectric refrigeration. *J. Phys. Chem. Solids*. 10 (2–3), 191–200. https://doi.org/10.1016/0022-3697(59)90074-5.

Rowe, D.M. (2005). *Thermoelectrics Handbook: Macro to Nano.* CRC Press, Boca Raton.

Snyder, G., Toberer, E. (2008). Complex thermoelectric materials. *Nature Materials* 7, 105–114. https://doi.org/10.1038/nmat2090.

Soni,A., Shen, Y., Yin, M., Zhao, Y., Yu, L., Hu, X., Dong, Z., Khor, K.A., Dresselhaus, M.S., Xiong, Q. (2012*)*. Interface driven energy filtering of thermoelectric power in spark plasma sintered $Bi_{(2)}Te_{(2.7)}Se_{(0.3)}$nanoplatelet composites. *Nano Lett*. 12 (8), 4305–4310. https://dx.doi.org/10.1021/nl302017w.

Wu, F., Song, H., Jia, J., Hu, X. (2013). Effects of Ce, Y, and Sm doping on thermoelectric properties of Bi_2Te_3 alloy. *Prog. Nat. Sci.: Mat. Inter*. 23 (4), 408–412. https://doi.org/10.1016/j.pnsc.2013.06.007.

Yan, X., Poudel, B., Ma, Y., Liu, W., Joshi, G., Wang, Y.,Lan, Y., Wang, D., Chen, G., Ren, Z. (2010*)*. Experimental studies on anisotropic thermoelectric properties and structures of n-type $Bi_2Te_{2.7}Se_{0.3}$. *Nano Lett*. 10 (9), 3373–3378. https://dx.doi.org/10.1021/nl101156v.